Universal properties of complexes formed by two oppositely charged flexible polyelectrolytes

Roland G Winkler

Institut für Festkörperforschung, Forschungszentrum Jülich,
52425 Jülich, Germany
E-mail: r.winkler@fz-juelich.de

Abstract. Results of molecular dynamics simulations for systems with two flexible, oppositely charged polymer chains are presented. It is shown that the chains aggregate into densely packed structures. The universal properties of the formed complexes are investigated as a function of chain length and interaction strength. For weakly interacting systems, a chain length-dependent effective interaction strength is obtained which governs the initiation of the aggregation process. At intermediate interaction strengths, the formed complexes exhibit a scaling behaviour with respect to molecular weight typically for chain molecules in a bad solvent. An unusual weak dependence of the radius of gyration on the interaction strength is found in this regime. Finally, for strong interactions, tightly packed globules are obtained. The radii of gyration and the densities of the complexes are discussed.

Contents

1. Introduction

Aggregates between oppositely charged macromolecules play a fundamental role in technical applications and in particular in biological systems. An example is DNA which is associated with histone proteins to form the chromatin. Recently, aggregates of DNA and cationic polymers [1]–[4] and cationic dendrimers [5]–[8] have attracted considerable attention. The reason is their potential application as DNA vectors in gene therapies.

Various investigations are underway to unravel the mechanisms leading to particular aggregates in charged systems. However, up to now, there is no clear understanding of the appearing structures. From a theoretical point of few, the long-range character of the Coulomb interaction renders such systems difficult to treat analytically. Nevertheless, various authors have studied the adsorption of polyelectrolytes onto charged surfaces theoretically [9]–[16] and a statistical theory for globular polyelectrolyte complexes has been presented also [17]. Computer simulations are an important tool for the detailed investigation of these systems on a molecular level. So far mostly chains with added counterions and colloidal systems have been studied [18]–[27]. Less attention has been paid to complexes formed by oppositely charged chains [28]–[33].

The aim of the simulations presented in this paper is to investigate the universal properties of aggregates formed by oppositely charged chain systems when they collapse, thereby forming compact cluster-like structures which are physically constrained to a small region in space. The simulations reach beyond previous ones, since we study systematically a large range of interaction strengths and chain lengths. In particular, we analyse the scaling behaviour of the chain conformations with respect to chain length and interaction strength. Our studies focus on two-chain systems. Hence, the results apply to the formation of chain-pairs in many-chain systems only. Such pairs form certainly in dilute systems, where the density is much smaller than the overlap concentration. In this limit, the behaviour of the solution is determined by the aggregates of two or only a few chains. Depending on the concentration of positively and negatively charged chains, all or only part of the molecules form pairs [30]. Larger aggregates are formed at polymer concentrations close to the overlap concentration. The behaviour of the solution is then determined by large globules.

The paper is organized as follows. In section 2 the system and the simulation method are described. In section 3 the results are presented. In particular, the dependence of the radius of gyration on the interaction strength between the chains and the chain length, respectively, is discussed. In addition, results for the density within a cluster are presented. Finally, section 4 summarizes our findings.

2. System and simulation method

We performed constant-temperature molecular dynamics simulations with two oppositely charged chain molecules [31]. A polymer chain is composed of mass points connected by harmonic bonds with the potential

$$V_B = \frac{\kappa}{2} \sum_{i=2}^{N} (|\boldsymbol{r}_i - \boldsymbol{r}_{i-1}| - l)^2. \tag{1}$$

To ensure small fluctuations in the bond lengths (below 1%), a large value for the force constant κ is chosen ($\kappa = 5000\epsilon/\sigma^2$, where ϵ and σ are the parameters of the Lennard–Jones potential, cf equation (2)).

The finite size of the monomers is taken into account by the truncated Lennard–Jones potential

$$V_{LJ} = \begin{cases} 4\epsilon\left[\left(\dfrac{\sigma}{r}\right)^{12} - \left(\dfrac{\sigma}{r}\right)^{6}\right] + \epsilon & \text{for } r < \sqrt[6]{2}\sigma, \\ 0 & \text{for } r > \sqrt[6]{2}\sigma, \end{cases} \tag{2}$$

where r denotes the distance between two (non-bonded) mass points. In our simulation we set the bond length $l = \sigma$.

In addition, all mass points interact via the Coulomb potential

$$V_C = \sum_i \sum_{j>i} \frac{z_i z_j e^2}{\varepsilon|\boldsymbol{r}_i - \boldsymbol{r}_j|}, \tag{3}$$

where ε is the electric permittivity and e the charge of an electron. The $z_i = \pm 1$ denote the charge state of the monomers. The interaction with the solvent is taken into account by a stochastic force ($\boldsymbol{\Gamma}_i$) and a friction force, with a damping constant γ, acting on each mass point. The equations of motion of the system are then given by the Langevin equations

$$m\ddot{\boldsymbol{r}}_i = \boldsymbol{F}_i - \gamma m\dot{\boldsymbol{r}}_i + \boldsymbol{\Gamma}_i \tag{4}$$

($i = 1, \ldots, N$). $\boldsymbol{F}_i$ comprises the force due to the potentials (1)–(3), and m is the mass of a point particle. The stochastic force is assumed to be stationary, random and Gaussian (white noise). This ensures the proper equilibration of the dilute system [34, 35].

The electrically neutral system is placed in a cubic simulation box and periodic boundary conditions are applied for the intermolecular Lennard–Jones interaction, thereby keeping the density ($\rho = N/V = 2.2 \times 10^{-7}/\sigma^3$) of the system constant when changing the chain length. This is only relevant for very low interaction strengths, where the chains are well separated. For sufficiently large interaction strengths, the chains form aggregates confining themselves in a small region in space. The number (N) of monomers per chain was chosen as $N = 10, 20, 40$, 80 and 160, to span at least one order of magnitude. Hence, it is possible to study the scaling behaviour of the system with respect to size at a given interaction strength for this length scale. In terms of the Lennard–Jones potential parameters (σ, ϵ), the (dimensionless) Coulomb interaction parameter λ is given by $\lambda = l_B k_B T/\epsilon\sigma$, where $l_B = e^2/\varepsilon k_B T$ is the Bjerrum length.[1] Hence, there are only two relevant parameters in our simulation, the length of the chains N and the interaction strength λ. λ is chosen in the range of $\lambda = 0, \ldots, 100$. This range covers uncharged chains in good solvent as well as highly charged chain systems. For the Coulomb interaction we use a cutoff R_c which is half the box length. This is possible because the eventually analysed collapsed systems are confined to a small region in space which is much smaller than R_c. For non-collapsed chains, the Coulomb interaction is sufficiently weak to be neglected beyond the cutoff distance. The temperature is chosen as $k_B T = 1.2\epsilon$, the damping constant as $\gamma = 1/\tau$ and the time step

---

[1] Alternatively, the interaction strength can be definite as $\tilde{\lambda} = l_B/\sigma$. Since we set $k_B T = 1.2\epsilon$, $\lambda = 1.2\tilde{\lambda}$.
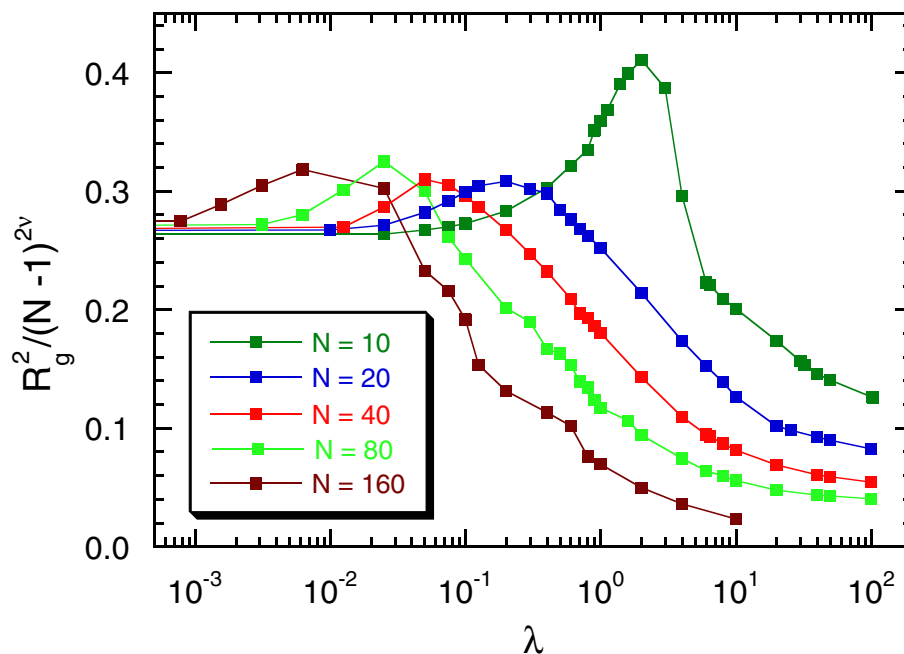
Figure 1. Radii of gyration as a function of interaction strength for various chain lengths. The exponent $\nu = 0.6$.

is $\Delta t = 5 \times 10^{-3}\tau$, where τ is the time unit of the simulation. To obtain reasonable statistics, at least 20 different initial conditions were considered and simulations up to 10^7 time steps were performed for each value of λ and N.

In addition, we performed simulations taking counterions into account. The results presented in the next section, however, do not depend on the presence of the counterions.

3. Results and discussion

3.1. Radius of gyration

As a consequence of the long-range nature of the Coulomb interaction, the two chains attract each other and form neutral complexes [31]. The aggregation process starts already at very low interaction strengths (λ). The reason is the large local charge density due to the presence of bonds. At very low densities, the Coulomb interaction is $\sim N^2$ for centre-of-mass distances much larger than the radius of gyration of a chain. As a consequence, the effective interaction among the chains is chain-length-dependent. This is obvious from figure 1, which displays the radii of gyration for various chain lengths. At small interaction strengths, the chains are free and the radii of gyration are equal to the values of chains in a good solvent. With increasing interaction strength, the chain extension increases slightly. Considering the scaling behaviour of the radius of gyration with respect to chain length, we find the same exponent as in a good solvent, i.e. the slight chain extension does not alter the scaling properties. Beyond a certain λ the chains form aggregates. The intramolecular Coulomb interaction is then screened and the chains shrink again. For large interaction strengths, the size of the chains is smaller than the size of a corresponding
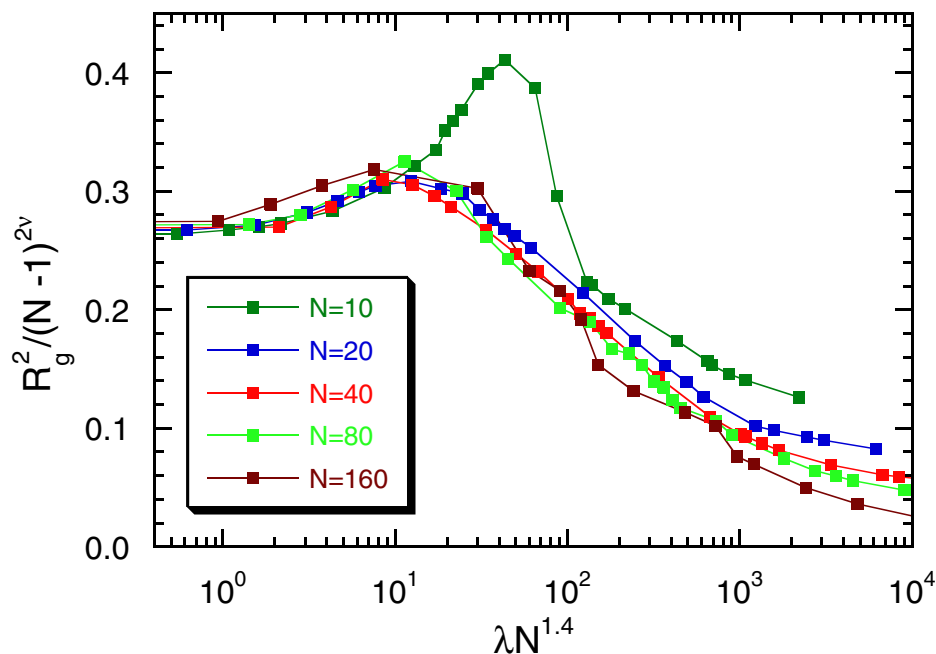
Figure 2. Radii of gyration as a function of the effective interaction strength $\lambda^* = \lambda N^{1.4}$ for various chain lengths ($\nu = 0.6$).

uncharged chain in a good solvent. There is evidently an attractive interaction in the system present, which gives rise to the compact structure.

The smallest chain systems with $N = 10$ do not fit into the scheme of the larger ones. For $N = 10$, the ratio $R_g^2/(N-1)^{2\nu}$ exceeds obviously the value for chains of length $N = 20$. A more detailed analysis exhibits two conformations for such chains ($\lambda \approx 1$): a rather collapsed state (globule) and a stretched state (double-stranded helix) [31].

When the Coulomb energy is of the order of $k_B T$, we expect the chains to stay close to each other with a mean distance comparable with the radius of gyration of a single chain. With the Coulomb energy $E_C \sim N^2/R_g \sim N^2/N^\nu$ the strength of the interaction is then estimated to be $\lambda_B N^\phi \approx 1$. Hence, we find an effective interaction strength $\lambda^* = \lambda N^\phi$, with $\phi = 2 - \nu = 1.4$, which governs the onset of the collapse of the formed aggregate. Figure 2 depicts R_g^2 as a function of λ^*. As is obvious from the figure, the data for various chain lengths collapse approximately onto a universal curve for $\lambda^* \lesssim 10$. There is a clear tendency of the systems to start collapsing approximately at the same value of $\lambda^* = \lambda_c^* \approx 10$.

Single polyelectrolyte chains in the presence of counterions exhibit a different behaviour [20]. Such chains also start to collapse at a certain interaction strength (λ) due to counterion condensation. However, the corresponding λ value is nearly independent of chain length. Considering the exponents (ν) for the mean-square end-to-end distance and the radius of gyration, respectively, for these systems, the exponents increase with increasing interaction strength until counterion condensation starts and the exponent for the mean-square end-to-end distance is close to $\nu \approx 1$, corresponding to rod-like chains. The chains in the two-chain system, however, are only weakly perturbed for $\lambda^* \lesssim 20$, because of the effectively small interaction strength λ. In particular, they are never stretched in a rod-like manner due to the screening of the intramolecular Coulomb interaction by the oppositely charged chain. For larger interaction parameters, the chains start to collapse and form dense clusters.
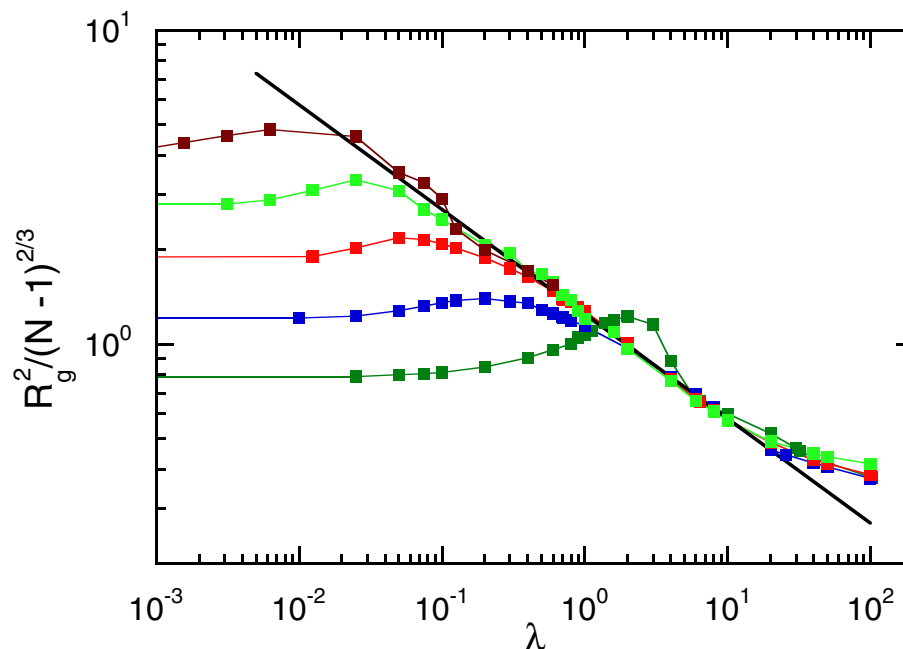
Figure 3. Radii of gyration of one chain as a function of the interaction strength for various chain lengths. R_g^2 is scaled by $(N-1)^{2/3}$, where $(N-1)$ is the number of bonds of a chain.

The critical effective interaction strength $\lambda_c^* \approx 10$ can be used to separate the one-phase state with scattered chains and the phase with a globule. For $\lambda^* < \lambda_c^*$ individual chains are present; in contrast, for $\lambda^* > \lambda_c^*$ the chains aggregate and fold into densely packed structures.

Another universal regime is obtained for intermediate interaction strengths λ. Figure 3 presents mean-square radii of gyration scaled by $(N-1)^{2/3}$, corresponding to the scaling behaviour of chains in a bad solvent, as a function of interaction strength. The curves for the various chain lengths nicely fall on top of each other for a broad range of interaction strengths, where the actual range depends on chain length. Our results are in agreement with some of the results obtained in [28]. Depending on the interaction strength, Srivastava and Muthukumar [28] find ν values in the range 0.35–0.5.

Evidently, we can extract a scaling relation for the dependence of the radius of gyration on the interaction strength from figure 3. The data for the various chain lengths follow the relation $R_g \sim \lambda^{-1/6}$ very well in the regime of intermediate interaction strengths. This is an unusual weak λ dependence and will be addressed in more detail below (section 3.3).

With increasing interaction parameter the chains ultimately form very compact, collapsed objects. The individual monomers are then closely packed and the radius of gyration is independent of the interaction strength. The chains behave in this regime like chains in a bad solvent with an almost constant density of the globule and the radius of gyration displays the dependence $R_g \sim N^{1/3}$.

3.2. Density

The change of the radius of gyration with the interaction strength is associated with a change of the density of the aggregate. For the chain lengths we have been studying, there is only a
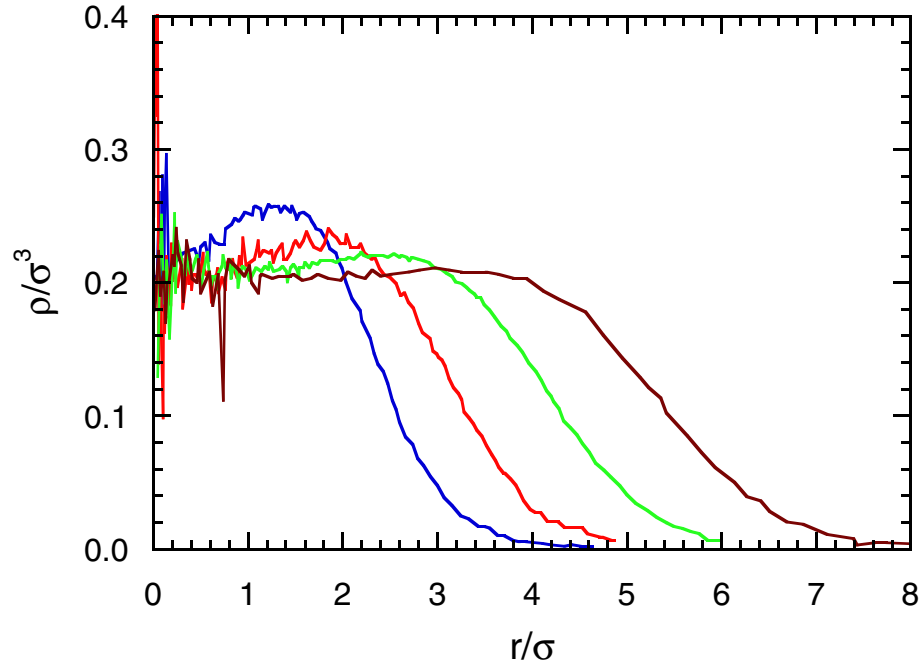
Figure 4. Radial density of monomers with respect to the centre of mass of a globule. The interaction strength is $\lambda = 4$. The colour code for the chain lengths is as in figure 1.

slight dependence of the density on the chain length for a given interaction strength in the regime $0.6 < \lambda < 20$. We even observe plateaux in the monomer densities for a particular interaction strength. Figure 4 presents an example for $\lambda = 4.0$. ρ measures the radial monomer density with respect to the centre of mass. The plateau-like regime is clearly present for long chains. For short chains we observe a pronounced maximum of the density. This maximum vanishes with decreasing interaction strength. On the other hand, such a maximum appears also at higher interaction strengths for longer chains. The reason for this is the geometry of the globule. Monomers on the outer part of the cluster experience an attractive interaction from inside the cluster and no interaction from outside. Thus, these monomers show a stronger attraction by the kernel part than monomers inside of the cluster. For smaller interaction strengths (or higher temperatures), chains of different lengths are deformed to different degrees (cf figure 1), which leads to a chain length dependence of the density profile.

From figure 3, we extract the dependence $R_g \sim N^{1/3}\lambda^{-1/6}$. Using the relation $\rho \sim N/V \sim N/R_g^3$ for the density dependence on the chain size, ρ changes with the interaction strength according to $\rho \sim \lambda^{1/2}$. Hence, the density increases with the interaction strength in a non-linear manner. From the calculated density profiles the dependence $\rho \sim \lambda^{0.4}$ is obtained. The latter exponent is smaller than the one predicted by the density argument. Considering the simplicity of the arguments used and the statistical uncertainties of the simulation results, which are reflected by the fluctuations of the curves, however, the relationship supports the dependence $R_g \sim \lambda^{-1/6}$. In particular, the exponent is not larger than $1/6$.

In [17] results for the density dependence of globular complexes on the interaction strength are provided for weakly interaction systems which deviate from the findings above [31]. Since the considered systems are different the observed differences may be reasonable. It
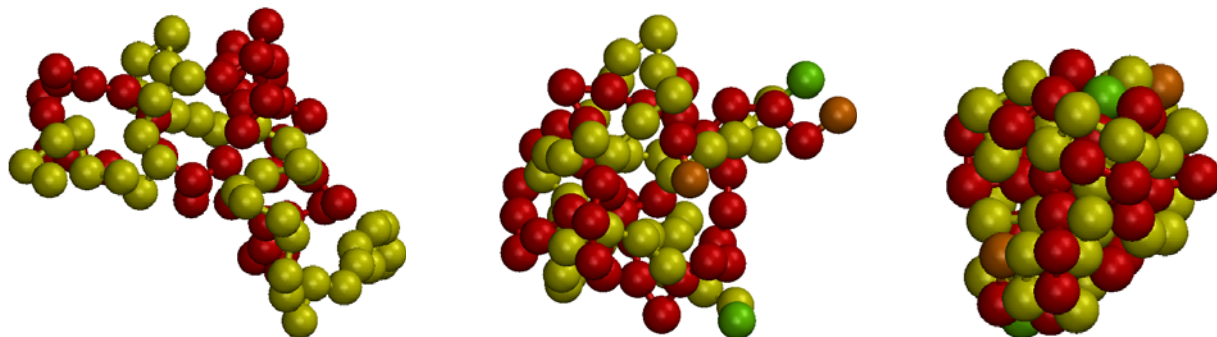
Figure 5. Snapshots of aggregates for chains of length $N = 40$ and the interaction strengths $\lambda = 0.4, 4, 40$ (from left to right).

remains to establish a link between the two-chain aggregates of this article and the globules discussed in [17].

Figure 5 provides a example for the aggregates formed at different interaction strengths. For the chain length $N = 40$ no compact structure is formed at $\lambda = 0.4$, although the radius of gyration of a chain is already smaller than in a good solvent (cf figure 1). At $\lambda = 4.0$ there is already a pronounced peak in the pair-correlation function at $r = 2\sigma$ indicating the formation of a denser structure [31]. A further increase of λ leads to an even more compact cluster. For very strong interactions, even crystalline-like structures are obtained locally [31].

3.3. Scaling considerations

The particular shape of an aggregate at a certain interaction strength is determined by the competition between an effective attractive interaction and the repulsion by the excluded volume of the monomers.

To gain insight into the aggregation mechanism, let us assume that the monomers can be redistributed such that a charge in the globule resembles a charge in a simple ionic solution. The electrostatic interactions create correlations such that any charge is surrounded by a shell of oppositely charged monomers. Thus, the Coulomb interactions are screened. As has been done before for a random polyampholyte [36], we will describe the aggregate in the same way as a system of free charges in an ionic solution and calculate the electrostatic energy of the aggregate as if it were a small volume of a Debye–Hückel electrolyte solution. The detailed calculation [36] yields the cluster size $R \sim N^{1/3}\lambda^{-1/3}$ for a θ solvent. Similarly, for the situation of a good solvent $R \sim N^{1/3}\lambda^{-2/3}$ is obtained. Calculations for a polyelectrolyte with condensed counterions with an effective interaction assuming randomly oriented dipoles yields similar dependences [37]. Using the relation $\rho \sim N/R^3$ the above cluster sizes correspond to the density dependences $\rho \sim \lambda$ (θ solvent) or $\rho \sim \lambda^2$ (good solvent). However, none of these results agree with the scaling relations we extracted from our computer simulation data. Both the dependence on R as well as on the density are different. One reason might be that the electrostatic screening is in the non-linear regime in the present system, whereas the predictions above are based on the linear Debye–Hückel theory. At the moment we cannot provide an explanation of the observed behaviour on the basis of scaling arguments. There is either a different kind of interaction present, which governs the system behaviour, or the clusters are so small that surface effects play

an important role. The scaling relations outlined above might then apply to much longer chains. Studies are in progress to resolve this issue.

4. Conclusions

Molecular dynamics simulation results of systems with two oppositely charged chains have been presented. For small interaction strengths, we find that similar structures for chains of various lengths are obtained for the effective interaction strength $\lambda^* = \lambda N^{1.4}$. In this regime the chains exhibit universal behaviour and we find scaling exponents for the radius of gyration and the end-to-end distance similar to the value for uncharged chains in a good solvent. For intermediate interaction strengths the chains form aggregates, whose sizes are smaller than the size of a chain in a θ solvent. The typical chain dimension scale (with respect to chain length) similar to those of a polymer in a bad solvent in this regime ($R_g \sim N^{1/3}$). As far as the dependence on interaction strength is concerned, we observe an unusual $R_g \sim \lambda^{-1/6}$ dependence, which is consistent with the observed interaction strength dependence of the density.

Standard arguments applied to polyampholytes and polyelectrolytes with condensed counterions do not account for the observed behaviour. Hence, it remains to be clarified what kind of interactions are responsible for the results found in the computer simulations.

For very strong interactions, the systems form very compact glass-like (for large enough λ) structures with a distinct round surface and pronounced local order. This occurs at all investigated chain lengths. Systems of various chain lengths exhibit again self-similarity on the small length scale. Collective phenomena play a major role in the formation of the observed structures, starting from the moment the chains begin to wind around each other, subsequently form helical-like structures, and finally fold into dense globules [31].

We presented results for two oppositely charged chains. We expect the observed behaviour to apply for dilute systems, where the density is much smaller than the overlap density. This is confirmed by Monte Carlo simulations in [30].

We have also performed simulations taking counterions into account. However, the aggregation process for intermediate and strong interactions was not affected by the presence of the counterions. The reason is the chain-length-dependent interaction strength. The interaction among the chains is so strong that they aggregate before counterion condensation starts. At higher interaction strengths, more likely counterion–counterion pairs are observed than counterion condensation, which is more favourable with respect to the translational entropy of the whole system.

Acknowledgments

References

[1] Felgner P L, Gadek T R, Holm M, Roman R, Chan H W, Wenz M, Northrop J P, Ringold G M and Danielsen M 1987 *Proc. Natl. Acad. Sci. U.S.A.* **84** 7413
[2] Hansma H G, Golan R, Hsieh W, Lollo C P, Mullen-Ley P and Kwoh D 1998 *Nucleic Acids Res.* **26** 2481
[3] Dunlop D D, Maggi A, Soria M R and Monaco L 1997 *Nucleic Acids Res.* **25** 3095

[4] Yamasaki Y, Teramoto Y and Yoshikawa K 2001 *Biophys. J.* **80** 2823
[5] Chen W, Turro N J and Tomalia D A 1999 *Langmuir* **16** 15
[6] Kabanov V A, Zezin A B, Rogacheva V B, Gulyaeva Zh G, Zansochva M F, Joosten J G H and Brackman J
       1999 *Macromolecules* **32** 1904
[7] Welch P and Muthukumar M 2000 *Macromolecules* **33** 6159
[8] Gössl I, Shu L, Schlüter A D and Rabe J P 2002 *J. Am. Chem. Soc.* **124** 6860
[9] Goeler von F and Muthukumar M 1994 *J. Chem. Phys.* **100** 7796
[10] Marky N L and Manning G S 1995 *J. Mol. Biol.* **255** 50
[11] Gurovitch E and Sens P 1999 *Phys. Rev. Lett.* **82** 339
[12] Mateescu E M, Jeppesen C and Pincus P 1999 *Europhys. Lett.* **46** 493
[13] Park S Y, Bruinsma R F and Gelbart W M 1999 *Europhys. Lett.* **46** 454
[14] Kunze K-K and Netz R R 2000 *Phys. Rev. Lett.* **85** 4389
[15] Kunze K-K and Netz R R 2002 *Europhys. Lett.* **58** 299
[16] Cherstvy A and Winkler R G submitted
[17] Borue V Yu and Erukhimovich I Ya 1990 *Macromolecules* **23** 3625
[18] Stevens M and Kremer K 1995 *J. Chem. Phys.* **103** 1669
[19] Stigter D 1995 *Macromolecules* **95** 380
[20] Winkler R G, Gold M and Reineker P 1995 *Phys. Rev. Lett.* **80** 3731
[21] Dobrynin A V and Rubinstein M 1996 *Macromolecules* **29** 2974
[22] Wallin T and Linse P 1996 *Langmuir* **12** 305
[23] Wallin T and Linse P 1996 *J. Phys. Chem.* **100** 17873
[24] Kong C Y and Muthukumar M 1998 *J. Chem. Phys.* **109** 1522
[25] Jonsson M and Linse P 2001 *J. Chem. Phys.* **115** 3406
[26] Messina R, Holm C and Kremer K 2002 *J. Chem. Phys.* **117** 2947
[27] Khalatur P G, Khokhlov A R, Mologin D A and Reineker P 2003 *J. Chem. Phys.* **119** 1232
[28] Srivastava D and Muthukumar M 1994 *Macromolecules* **27** 1461
[29] Imbert J B, Victor J M, Tsunekawa N and Hiwatari Y 1999 *Phys. Lett.* A **258** 92
[30] Hayashi Y, Ullner M and Linse P 2002 *J. Chem. Phys.* **116** 6836
[31] Winkler R G, Steinhauser M O and Reineker P 2002 *Phys. Rev.* E **66** 021802
[32] Hayashi Y, Ullner M and Linse P 2003 *J. Phys. Chem.* B **107** 8198
[33] Dias R S, Pais A A C C, Miguel M G and Lindman B 2003 *J. Chem. Phys.* **119** 8150
[34] Winkler R G, Ludovice P J, Yoon D Y and Morawitz H 1991 *J. Chem. Phys.* **95** 4709
[35] Risken H 1989 *The Fokker–Planck Equation* (Berlin: Springer)
[36] Higgs P G and Joanny J-F 1991 *J. Chem. Phys.* **94** 1543
[37] Schiessel H and Pincus P 1998 *Macromolecules* **31** 7953